

Local Order in Depolymerized Silicate Lattices

Graciela Pacheco-Malagón,[†] Patricia Pérez-Romo,^{*‡} Norma A. Sanchez-Flores,[†]
 María L. Guzmán-Castillo,[‡] Carlos López,[‡] José M. Saniger,[†] Francisco Hernández-Beltrán,[‡] and
 José J. Fripiat^{†‡}

Centro de Ciencias Aplicadas y Desarrollo Tecnológico, Cd. Universitaria AP 70-186,
 C.P. 04510 México, D.F., and Instituto Mexicano del Petróleo, Eje Central Lázaro Cárdenas,
 152, Col. San Bartolo Atepehuacan, C.P. 07730 México, D.F.

Received April 11, 2005

In glycerol, near 200 °C, the silicate networks of mesoporous silicates and zeolites undergo a deep depolymerization process. In a few hours, depending on the initial concentration of the solid in glycerol and on the temperature, amorphous gels are obtained. In these gels, a fraction of the Si–O–Si bonds are transformed into Si–O–C. The constitutional aluminum remains bound to the silica network in the gel. The short range ordering is maintained to some extent: the size of the smallest structural unit in gels obtained from zeolites is in the range of the cubic nanometer, nm³.

Introduction

The silicates, which are the main constituents of earth crust, are quite resistant to chemical agents operating in a moderate pH range. For instance, in water, 140 ppm silica is dissolved at room temperature, and the solubility is even lower in alcohols. The origin of this work is the observation that crystalline mesoporous silicas, such as MCM-41^{1–3} or FSM-16,^{4–6} dissolve rapidly below 200 °C in glycerol forming soft gels or viscous liquids, depending on the reaction conditions. The solubility of the organo-complex in glycerol is in the percent range, that is to say, more than 10000 times the solubility in water. The silica network is depolymerized. The gel is X-ray amorphous. Thus, the

probability of a silicon tetrahedron sharing its four corners with identical tetrahedra is statistically and significantly lowered.

High surface area xerogel,⁷ synthetic acid faujasite HY,^{8,9} a member of the MF1 group, H-ZSM5,^{8–9} acid Clinoptilolite,¹⁰ a member of the Heulandite family, can be jellified as well. The depolymerized material is similar to a hyper-branched silicon alkoxide, the depolymerization reaction proceeding by a condensation process between a silanol group and an alcohol function of glycerol, liberating water (etherification). In zeolites, the fate of the constitutional aluminum, and, in particular, its coordination, deserves special consideration.

The structures of silicates may be quite complicated, but the essential building block is the Si tetrahedron of symmetry *T_d*. Long-range order is revealed by the interference based techniques, such as X-ray or neutron diffraction. Local ordering is approached by IR spectroscopy, or by MAS NMR.

The efficiency of the depolymerization process can be appreciated by the ratio C/Si characteristic of the final product.

* To whom correspondence should be addressed. E-mail: pperezr@imp.mx.

[†] Centro de Ciencias Aplicadas y Desarrollo Tecnológico.

[‡] Instituto Mexicano del Petróleo.

- (1) Kresge, C. T.; Leonowicz, M. E.; Roth, W. J.; Vartuli, J. C.; Beck, J. S. *Nature* **1992**, *359*, 710.
- (2) Beck, J. S.; Vartulli, J. C.; Roth, W. J.; Leonowicz, M. E.; Kresge, C. T.; Schmitt, K. D.; Chu, C. T. W.; Olson, D. H.; Sheppard, E. W.; McCullen, S. B.; Higgins, J. B.; Schlenker, J. L. *J. Am. Chem. Soc.* **1992**, *114*, 10834.
- (3) Beck, J. S.; Vartulli, J. C.; Kennedy, G. C.; Kresge, C. T.; Roth, W. J.; Schramm, S. E. *Chem. Mater.* **1994**, *6*, 1816–1821.
- (4) Yanagisawa, T.; Shimizu, T.; Kurado, K.; Kato, C. *Bull. Chem. Soc. Jpn.* **1990**, *63*, 988.
- (5) Chen, C.-Y.; Xia, S.-Q.; Davis, M. E. *Microporous Mater.* **1995**, *4*, 1.
- (6) Pérez-Romo, P.; Guzmán-Castillo, M. L.; Armendáriz-Herrera, H.; Navarrete, J.; Acosta, D. R.; Montoya, J. A. *Langmuir* **2003**, *19*, 3446–3452.

(7) Poncelet, G. Personal communication.

(8) Baerlocher, Ch.; Meier, W. M.; Olson, D. H. *The Atlas of Zeolite Framework Types*, 5th revised ed.; Elsevier: New York, 2001.

(9) Treacy, M. M. I.; Higgins, J. B. *Collection of Simulated XRD Powder Patterns for Zeolites*, 4th ed.; Elsevier: New York, 2001.

(10) Iler, R. K. *The Chemistry of Silica*; J. Wiley and Sons: New York, 1979.

The solubility of silica in various protic solvents has been investigated, but the last edition of the classical text *Chemistry of Silica* by R. K. Iler¹⁰ contains very few references to the solubility in alcohols, and a recent literature search does not contain reference to glycerol.

From the fundamental point of view, the local organization in X-ray amorphous gels is interesting for it shows that some characteristic features of the starting material are still observable in the gel, for instance in the ²⁹Si and ²⁷Al high-resolution NMR spectra. This observation opens the way to practical applications by the possibility of transforming a "cheap" structure into a more valuable one by a secondary synthesis operating on a gel having a correct Si/Al ratio. This research is in development and will be treated separately.

Experimental Section

1. Materials. Preparation of MCM-41 and of FSM-16. The synthesis procedure of MCM-41 was that described by Kresge et al.,¹ using CTAB as surfactant and an aging hydrothermal treatment at 100 °C for 6 days. The solid was finally calcined at 540 °C and identified by X-ray small angle scattering, NMR, and IR. The synthesis of FSM-16 has been described.⁶ From the point of view of the XRD resolution, the quality of the home-prepared MCM-41 and FSM-16 was comparable to those presented in the original works.^{2,4} The same general remark applies to the ²⁹Si MAS NMR spectra of the mesoporous silicas and zeolites. The X-ray diffraction (XRD) patterns of the zeolites materials used in the present work were also correctly identified.^{11–12}

The nomenclature used to designate the Qⁿsilicon clusters in these materials was that proposed by Engelhardt and Michel.¹³ It may be useful to recall that the Si chemical shift is sensitive not only to the coordination but also to the Si–O bond length and Si–O–Si bond angle. The presence of silanols is easily evidenced by cross-polarization. The deconvolution of the ²⁹Si MAS NMR spectra of the starting materials used in this work is shown in Table 1. The limitations of deconvolution techniques applied to the NMR spectra of imperfect or amorphous solids and gels are well-known. However, the repetitions of experiments carried out on materials with well documented characteristics, not only reproduced constantly the same features but also fit into expected quantitative correlations with data obtained from IR spectroscopy.

Xerogel. This phyllo-silica, in the sense defined by Iler,¹⁰ was obtained by removing completely, by acid leaching, the octahedral layer of phlogopite, a magnesium three-octahedral mica.⁷ The resulting solid was dried at 100 °C. The specific surface area was 430 m²/g. The average pore diameter was 3.6 nm and was determined by the BJH method. The hydration water, 8.7% w/w for a sample hydrated in atmosphere is removed below 200 °C, leaving behind silanol groups which are eliminated above 400 °C. The corresponding weight loss is 5.5%.

Synthetic Zeolites. Synthetic zeolites were provided by Zeolite International under the label CBV720 for HY and CBV5020 for H-ZSM5. The chemical compositions are shown in Table 2. The ²⁹Si MAS NMR spectra¹⁴ are well documented, and the result of

Table 1. Deconvolution (in Gaussians) of the ²⁹Si NMR Resonance Lines^a

Mesoporous Silicas and Xerogel									
MCM-41			FSM-16			xerogel			assign
δ (ppm)	W (ppm)	int (%)	δ (ppm)	W (ppm)	int (%)	δ (ppm)	W (ppm)	int (%)	
−107.5	10.3	74.0	−108.3	14.9	88.3	−113.9	9.0	61.0	Q ⁴
−99.3	6.7	23.4	−99.1	5.8	6.6	−103.9	7.7	32.7	Q ³
−91.2	5.5	2.5	−92.1	9.4	5.2	−94.6	6.2	6.0	Q ²
Synthetic Zeolites									
HY			HZSM-5						
δ (ppm)	W (ppm)	int (%)	δ (ppm)	W (ppm)	int (%)	assign			
			−115.6	3.24	20.8	Q ⁴			
			−112.4	3.62	53	Q ⁴			
−107.4	1.84	97.3	−108.6	10.4	26.2	Q ⁴			
						Q ³			
−101.6	2.06	6.3				Q ³			

^a Chemical shift (shift), full-width half-medium (W, ppm), and relative intensity (int, estimated error limits 5%). Assignments from ref 13.

Table 2. Chemical Analyses of the Starting Materials

component	clinop.SM	HY	H-ZSM5
SiO ₂	69.23%	78.9%	93.3%
Al ₂ O ₃	11.27%	5.3%	3.6%
Fe ₂ O ₃	1.42%		0.18%
MgO	0.6%		
CaO	2.11%		
Na ₂ O	0.64%		
K ₂ O	4.69%		
H ₂ O	10.64%	17.8%	3.1%
Si/Al	2.6 ^a	12.5	22.2

^a Theoretical value: 3.5–4.1.

the deconvolution is shown in Table 1. In HZSM-5, there are two different Q⁴ (0Al) sites at the origin of the lines at −115.6 and −112.4 ppm, in addition to the Q³ (1Al) line at −108.6 ppm, in agreement with Engelhardt and Michel.¹³ The well crystallized parent material (orthorhombic) silicalite contains 12 different crystallographic T sites. Attempts to correlate the NMR ²⁹Si line to these sites have been partially successful. The line widths in poorly organized zeolitic materials and the spreading of the lines on about 7 ppm prevent an accurate analysis. Moreover, calculation by molecular dynamics simulation of the charge on every silicon atom has shown that several tetrahedral sites can contribute to a single line.¹⁵

Natural Zeolite. Clinoptilolite, obtained from a raw material mined in San Luis Potosi, Mexico, was identified by XRD. The main impurities are, in decreasing abundance, quartz, cristobalite, albite, and microcline. From the intensity of the Bragg reflections, it was estimated that the raw material contains at least 50% clinoptilolite.

After ball-milling, the material was exchanged with a 0.1 M NH₄-Cl solution several times at room temperature and washed and purified several times by decantation. This product will be called clinoptilolite starting material and abbreviated as clinop.SM. Clinoptilolite is the sole cation exchanger detected in the mixture of minerals present in the raw material.

Crystallographically different Q⁴ (0Al) sites have been reported for this zeolite, but no detailed analysis has been offered.¹³ Taking

- (11) Sanchez, N. A.; Saniger, J. M.; d'Espinose de la Caillerie, J. B.; Blumenfeld A. L.; Fripiat, J. J. *J. Catal.* **2001**, *201*, 80–88.
 (12) Sanchez, N. A.; Saniger, J. M.; d'Espinose de la Caillerie, J. B.; Blumenfeld A. L.; Fripiat, J. J. *Mesoporous Microporous Mater.* **2001**, *50*, 41–52.
 (13) Engelhardt, G.; Michel, D. *High-Resolution Solid-State NMR of Silicates and Zeolites*; J. Wiley and Sons: New York, 1987.
 (14) Sanz, J.; Serratos, J. M. *J. Am. Chem. Soc.* **1984**, *106*, 4790.

- (15) Martinez Morales, E.; Fripiat, J. J.; Alvarez, L. J. *Chem. Phys. Lett.* **2001**, *349*, 286.

Table 3. Synthesis of the Gels^a

label	precursor	init conc (g/mL)	T (°C)	time (h)	yield (%)	silica in gel (%)
gel 2	MCM-41	0.025	240	2		
gel 3	MCM-41	0.05	240	2	21.6	55.5
gel 4	MCM-41	0.1	240	1	3.8	
gel 9	MCM-41	0.01	180	1	6.1	39.7
gel 10	MCM-41	0.01	180	2	6.1	37.4
gel 11	MCM-41	0.01	180	3	3.8	35.9
gel 15	MCM-41*	0.05	200	1	16.9	65.6
gel 17	FSM-16*	0.05	200	1	19.9	55.2
gel-45	xerogel	0.2	180	1.5	17.9	77.1
gel 32	clinop.SM	0.025	240	1		
gel 23	HY	0.1	200	2.5	71.2	66.9
gel23B	HY	0.1	200	1.5	58.3	63.0
gel 25	HZSM5	0.1	200	1.75	60	71.2

^a Experimental conditions: initial concentration (init conc) in g precursor/mL glycerol, temperature of reaction, and time. Final composition: yield of the reaction, or w/w % gel admixed with the solvent and w/w % silica in the gel.

into account the relatively high Si/Al ratio, Table 2, the presence of a strong Q³ (1Al) contribution is probable.

FT-IR spectra of self-supporting films of clinop.SM dehydrated under vacuum at 350 °C show the deformation bands of NH₄⁺ and of H₂O at 1430 and 1630 cm⁻¹, respectively. The hydration water disappears around 400 °C, and ammonia disappears at 600 °C. The Si/Al atomic ratio, from the overall chemical analysis, is 2.6. This value is lower than that calculated from the theoretical structural formula because of the partial dissolution of the feldspar impurities. The total chemical analyses are in Table 2. The theoretical composition of this member of the heulandite family is {28 Si, 8 Al} {4 Ca, 24 H₂O}.⁸ JCPD gives {29 Si, 7 Al} {K, 2 Na, 2 Ca, 24 H₂O}.

2. Experimental Techniques. All samples were equilibrated with atmospheric moisture before being characterized.

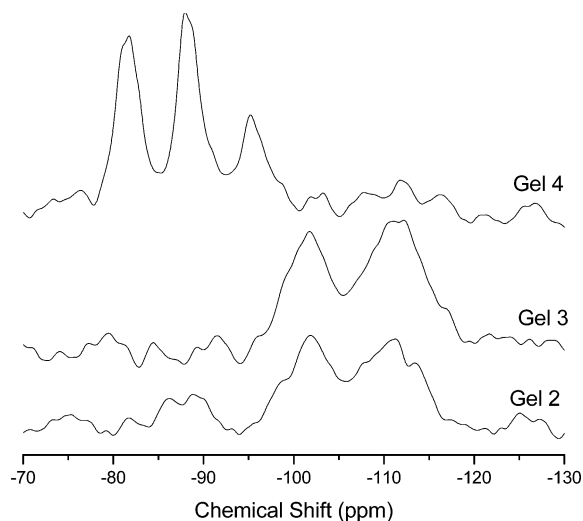
The XRD patterns of the crystalline silicates were recorded with a D-500 SIEMENS instrument fitted with a graphite secondary beam monochromator filtering the Cu Kα₁ radiation. The 2θ region from 1.5° to 10° was scanned by 0.02° steps and step time of 2 s.

The ²⁹Si MAS NMR spectra were obtained at 79.492 MHz, while spinning at 7.5 kHz with zirconia rotors, 4 mm i.d., and 90° pulses with 20 s intervals were used. The number of transients was 250 in all cases. ¹³C NMR experiments were recorded from 40 to 100 ppm at 100.6 MHz, while spinning at 6 kHz, with 4 μs pulse and 5 s intervals. ²⁷Al MAS spectra were recorded at 104.3 MHz with 12° pulses and 1 s intervals between pulses. The spinning rate was usually 10 kHz, and the number of transients was 300. The deconvolution of the NMR and FT-IR spectra was achieved by using the Origin 7 Windows software.

The FT-IR spectra were recorded with a Nicolet 5SX fitted with a CsI optic from a KBr window coated with the gel.

Thermal techniques, TGA, DTG, and DSC have been carried out with a Jupiter Netzsch STA 449C for carbon determination at a constant heating rate of 10 °C/min.

Depolymerization (Jellification) Procedure. The preparation of the gels was carried simply by stirring vigorously the starting material (SM) in glycerol at temperatures near 200 °C, for periods of time up to 3 h, as detailed in Table 3. Note that the gel contains all the silica present in the precursor, the organic material coming from the reaction with glycerol. It is dissolved in an excess glycerol. The gels' compositions obtained from the chemical analyses, described later, are shown by anticipation in Table 3 also. Depending on the gel concentration in the solvent, the final physical

**Figure 1.** ²⁹Si MAS NMR spectra corresponding to gels 2, 3, and 4.

aspect is between that of a soft solid and that of a viscous liquid that barely flows, after cooling at room temperature.

Experimental Results

Structural Aspect. Crystalline MCM-41 dissolves readily in glycerol. The so-called gels are X-ray amorphous, but the molecular structure can be established by ²⁹Si NMR.

Typical ²⁹Si MAS NMR spectra of three gels obtained under different experimental conditions are shown in Figure 1. Gel 4 obtained after a shorter reaction time, Table 3, is liquid while gels 2 and 3 are soft solids. The maximum intensity corresponding to the Q⁴ cluster with a resonance line between -110 and -114 ppm is observed in gels 2 and 3 but not in the liquid gel 4. The ²⁹Si resonance in the Q³ cluster, (SiO)₃SiOH, observed between -99 and -100 ppm in MCM-41 and FSM-16, Table 1, is shifted near -101.5 ppm and obviously enhanced in gels 2 and 3.

The ²⁹Si MAS NMR spectrum of gel 4 is very different. New signals between -80 and -95 ppm replace those observed in the less depolymerized gels. The ²⁹Si MAS NMR spectra of the starting materials (SMs) are characteristic of poorly crystallized material, resulting in broad resonance lines and severe overlaps of the various components. Yet the modifications shown in Figure 1 render the depolymerization process obvious.

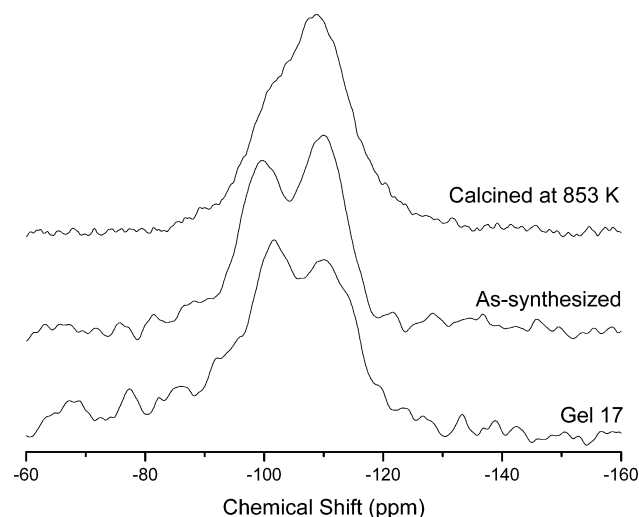
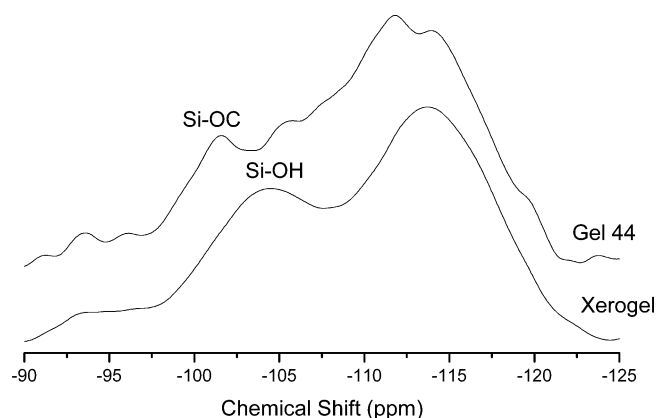
The comparison between gel 17 and the SM FSM-16, in Figure 2, confirmed the observations made for the soft gels 2 and 3. A similar comparison, between the spectra of the xerogel and of the derived gel 44, is represented in Figure 3. Table 4 contains the results of the ²⁹Si NMR spectra deconvolution in Gaussians for gels 2, 3, 4, and 44. In these gels, the absolute amount of Si-O-C is high, and the corresponding resonance should be observed easily. Accordingly, the intensity associated with the (SiO)₃SiOH Q³ cluster should decrease. Unfortunately, the spectral resolution does not allow the observation of these transformations.

In the case of gel 45 only, the Q³ resonance seems to split into two components, the downfield one being assigned tentatively to Si-O-C. In gels 2 and 3, such a splitting is not detectable, maybe because of the line width. A change

Table 4. Deconvolution of the ^{29}Si NMR Spectra of the Gels Prepared from MCM-41 and from Xerogel^a

gel 4			gel 3			gel 2			gel 44			assign
δ (ppm)	<i>W</i> (ppm)	int (%)	δ (ppm)	<i>W</i> (ppm)	int (%)	δ (ppm)	<i>W</i> (ppm)	int (%)	δ (ppm)	<i>W</i> (ppm)	int (%)	
						-114.3	1.9		-113.9	8.6	51.6	Q ⁴ 3D
			-111.3	8.3	62.7	-110.6	7.2	62.0	-106.5	10.6	36.	Q ⁴ 3D
-95.3	4.7	23.1	-101.4	5.6	37.1	-101.7	6.2	37.0	-101.8	5.1	11.2	Q ³ 3D
									-97.7	3.5	1.1	Q ³ 2D
-88.3	3.3	40.3				-89.5	2.8	6.1				Q ² 3D
												Q ² 2D
-81.6	3.3	36.5				-86.5	3.3	6.4				Q ² 3D

^a Chemical shift (shift), full-width half-medium (*W*, ppm), and integrated intensity (int, %). Assignment (assign) and dimensionality (D) according to refs 13 and 14.

**Figure 2.** ^{29}Si MAS NMR spectra of the as-synthesized and calcined at 863 K FSM-16 materials and of gel 17.**Figure 3.** ^{29}Si MAS NMR spectra of the xerogel and of gel 44, obtained after 2.5 h of reaction time.

of dimensionality from 3 to 2, that should be confirmed independently, is also suggested in Table 4 for gel 4 since no line has a chemical shift lower than -95 ppm.¹⁴ Consequently, under the conditions of poor resolution, inherent to the amorphous material studied here, the structural information obtained from ^{29}Si NMR is necessarily limited to recognize the depolymerization reaction. An attempt, so far unsuccessful, has been made to go further in comparing the chemical shift and intensity to those obtained in high resolution studies of trimethoxysilane polymerization in ethanolic solutions, such as that published by Dong et al.¹⁶

Table 5. Deconvolution of the ^{29}Si NMR Spectra in Gels Prepared by Depolymerizing Synthetic Zeolites^a

gel 23			gel 23B			gel 25			assign
δ (ppm)	<i>W</i> (ppm)	int (%)	δ (ppm)	<i>W</i> (ppm)	int (%)	δ (ppm)	<i>W</i> (ppm)	int (%)	
						-117.1	4.5	12.8	Q ⁴
-107.6	3.3	52.8	-107.7	4.2	82.2	-113.3	5.9	72	Q ⁴
-101.9	6.6	47.2	-102.4	3.2	17.8	-106.2	9.6	14.2	Q ³

^a Chemical shift (shift) and full-width half-medium (*W*, ppm), and relative intensity (int).

It is worth outlining that a structure similar to that of the starting MCM-41 has been recovered from gel 3, using Mokaya's high temperature secondary crystallization procedure.¹⁷ This claim is based on the observation of a d_{100} reflection at 4.62 nm, typical of a ^{29}Si NMR spectrum and of a characteristic N_2 adsorption isotherm. Hence, the depolymerization reaction is partially reversible in the presence of a structure-directing agent.

The ^{29}Si MAS NMR and ^{27}Al MAS NMR spectra of the synthetic zeolites and their gels are shown in Figures 4 and 5. It is remarkable to observe that the splitting of the Q⁴ (0Al) line in HZSM-5, Table 1, is maintained qualitatively in gel 25, Table 5. This observation indicates that some medium range ordering in the starting material is preserved in the amorphous gel.

In samples 23 and 23B, the intensity of the line assigned to Q³ has increased when compared to that of the starting material. Such an increase supports the extension of the suggested etherification reaction to zeolites. The effect of the duration of the reaction is well marked by the difference between gels 23 (2.5 h) and 23B (1.5 h). After 1.5 h reaction, the gel concentration in the solvent (Table 3) is smaller. More generally, the initial solid phase has often disappeared in less than 1 h at 200 °C.

In HY, Figure 4, the Al substitutions contribute to the intensity of the Q³ resonance at about -102 ppm well separated from the Q⁴ contribution near -107 ppm. In the gel obtained after 2.5 h reaction in glycerol at 200 °C, the relative intensity of the Q³ resonance is reinforced (Tables 1 and 5) suggesting an enhancement of the Si–O–C contribution, as in the gels obtained from MCM-41. Also

(16) Dong, H.; Lee, M.; Thomas, R. D.; Zhang, Z.; Reidy, R. F.; Mueller, D.W. *J. Sol-Gel Sci. Technol.* **2003**, *28*, 5.

(17) Mokaya, R. *J. Phys. Chem. B* **1999**, *103*, 10204.

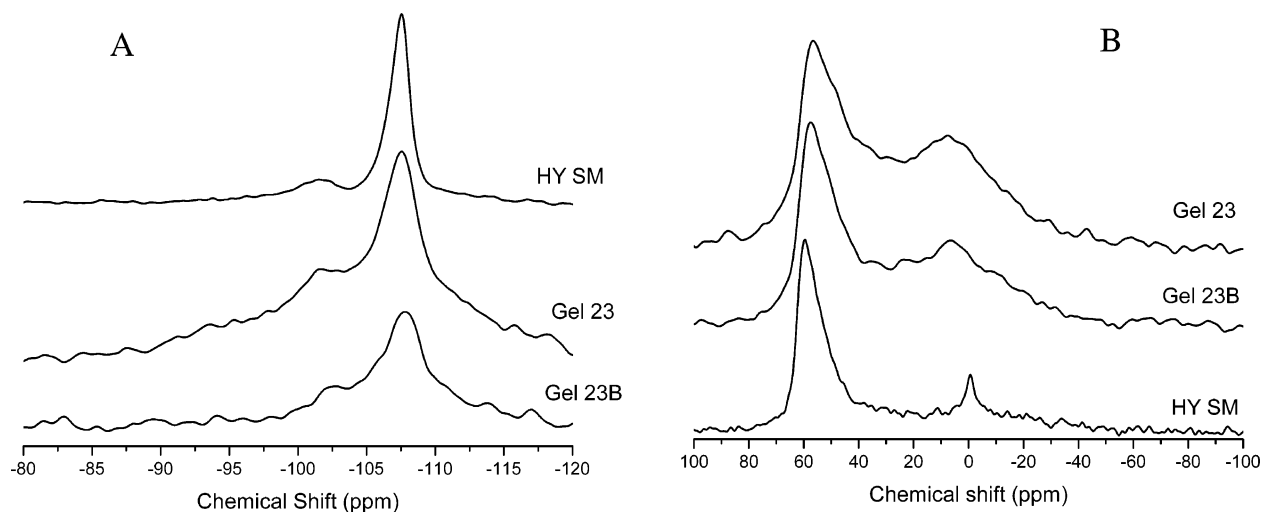


Figure 4. ^{29}Si (A) and ^{27}Al (B) MAS NMR spectra of HY and of gels 23 and 23B.

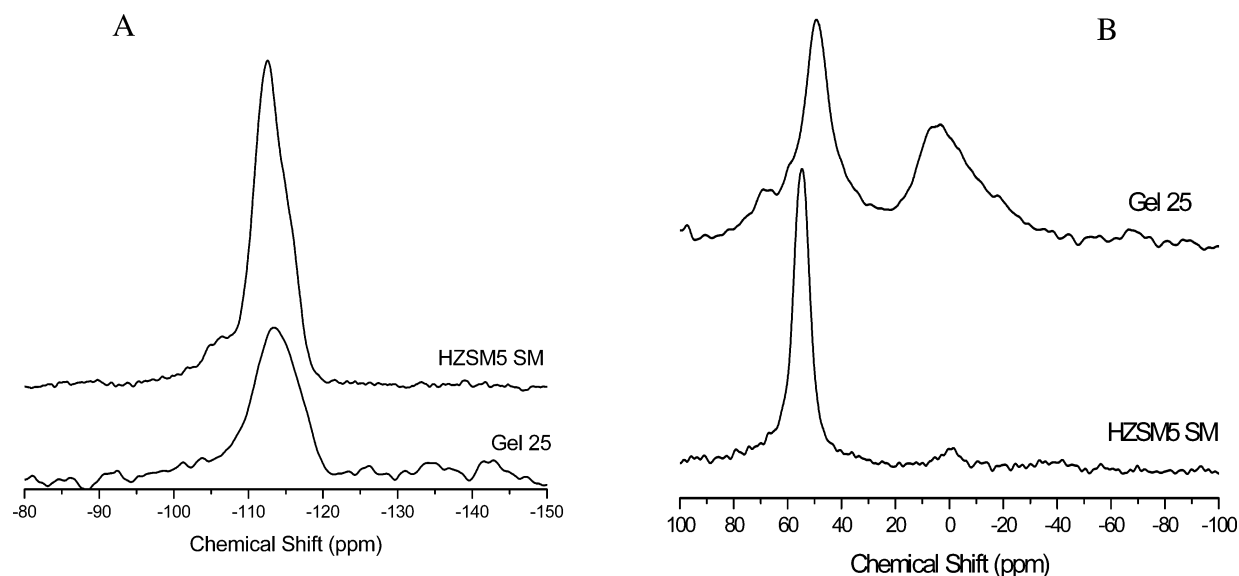


Figure 5. ^{29}Si (A) and ^{27}Al (B) MAS NMR spectra of HZSM-5 and of gel 25.

note in these tables that the Si resonance line widths are broader in the gels than in the SM, indicating a higher structural disorder, as anticipated.

Aluminum in the Gels. The ^{27}Al MAS NMR spectra are shown in Figures 4 and 5. In HY, Figure 4, a weak resonance at 0 ppm indicates the presence of some extra-framework, octahedral aluminum, as usually observed in acid HY.¹¹ The amount of octahedral aluminum increases significantly in the gel while the tetrahedral contribution decreases and the resonance lines broaden. Thus, some of the aluminum cations originally in tetrahedral coordination, and separated from one another in the silicate network (Lowenstein rule), are hydrolyzed and concentrated in aluminum “nests”, dispersed within the silica framework. This observation is repeated qualitatively in gel 25, derived from HZSM5, Figure 5, but the initial Si/Al ratio is about double that in HY. The line assigned to $\text{Q}^3(1\text{Al})$ has lost more than 50% of the initial intensity. Since the contributions $\text{Q}^3(\text{O}-\text{C})$ and $\text{Q}^3(\text{OAl})$ seem to have comparable chemical shifts, the loss of framework aluminum is probably even larger in gel 25.

The ^{29}Si MAS NMR and ^{27}Al MAS NMR spectra of

clinop.SM and of the viscous gel 32 are compared in Figure 6. Because of the mineralogical complexity, the ^{29}Si spectra are broad and the multiple components are poorly defined. Deconvolution into six Gaussian peaks has been attempted with reference to the major peaks in zeolites. Severe overlaps do not permit clear conclusions.

By contrast, the ^{27}Al spectra in Figure 6 are much simpler. The single singularity is a broad peak centered at about 52 ppm in the gel and 55 ppm in SM; the latter is broader than the former. Clinoptilolite, as well as the feldspars, augite and microcline, impurities have tetrahedral aluminum only. Gel 32 contains Si by Al substitutions in tetrahedral position.

Chemical Aspect. The representative IR spectra of gel 17 and gel 44 are compared in Figures 7 and 8. In particular, the comparison between FSM-16 and gel 17, Figure 7, delineates fairly well the inorganic from the organic contribution^{18,19} between 1500 and 1300 cm^{-1} . Frequencies and

(18) Bradley, D. C.; Multani, R. K.; Wardlaw, W. *J. Chem. Soc.* **1958**, 126, 4153.

(19) Guertin, D. L.; Stephen, E. W.; Bauer, W. H.; Goldenson, J. *J. Phys. Chem.* **1956**, 60, 1018.

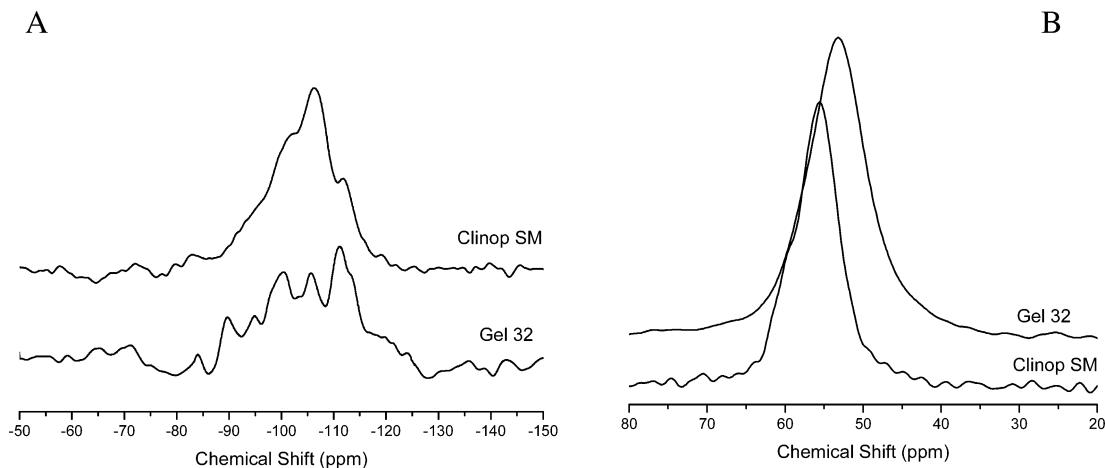


Figure 6. ^{29}Si (A) and ^{27}Al (B) MAS NMR spectra of clinoptilolite SM and of gel 32.

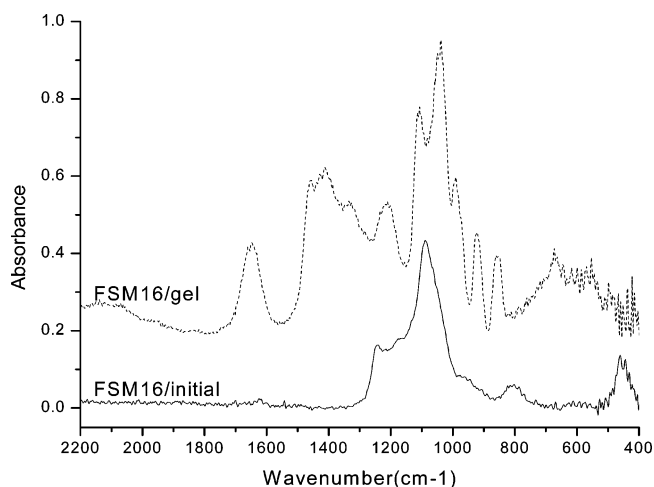


Figure 7. FT-IR spectra of the starting material FSM-16 and of the corresponding gel 25.

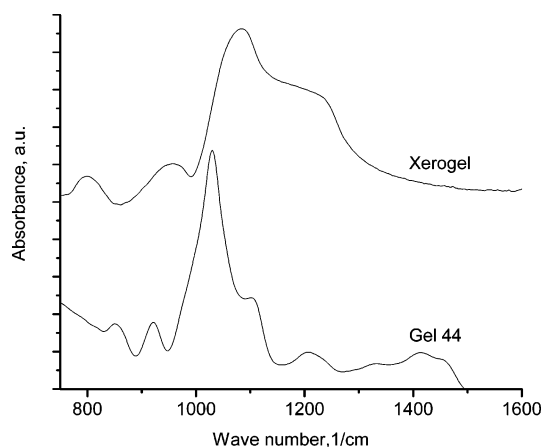


Figure 8. FT-IR spectra of xerogel and of the corresponding gel 45.

normalized intensities are in Table 6. These data were compared to the results of an exhaustive study of the infrared spectra of silicagels, obtained by hydrolysis of TEOS under various pH conditions, and of related structural data, Si–O bond lengths and Si–O–Si bond angles, obtained from the radial distribution.²⁰

(20) Fripiat, J. J.; Leonard, A.; Barake, N. *Bull. Soc. Chim. Fr.* **1963**, 122.

Table 6. IR Spectra Deconvolution^a

MCM-41		gel 3		gel 44		assign
ν (cm^{-1})	Nabs (%)	ν (cm^{-1})	Nabs (%)	ν (cm^{-1})	Nabs (%)	
943.7	7.8	945.9	1.15	927.1	21.8	n.a.
1047	15.5	1045	22.6	1029.3	49.3	Si–OH, ν_4
1099	27.1	1097	10.2	1104	13.6	Si–O, ν_3
1162.5	16.4	1161	5.3			Si–O
1230	17.1	1219	3.12	1202	14.6	Si–O

^a Wavenumber (ν , cm^{-1}), and normalized integrated absorbance (Nabs, %), are given for the starting MCM-41 and two gels.

Four frequencies at 1047 ± 3 , 1105 ± 10 , 1156 ± 3 , and $1205 \pm 10 \text{ cm}^{-1}$, were assigned to four stretching modes, ν_4 , ν_3 , ν_2 , and ν_1 , respectively. It was suggested that the intensity of ν_4 could be a trustable measurement of the substitution of oxygen by silanol or by O–C substitutions, both kinds of substitution resulting in an increase of the Si–O distance. The stretching frequency is an inverse function of the power of the internuclear distance: $\nu = Ad^{-n}$, n being usually between 2 and 3.²¹

Among the supporting experimental arguments, it was observed that ν_4 is lacking in the IR spectra of quartz, cristobalite, or tridymite, whereas the other frequencies, listed above, are easily observed.²⁰ A more recent discussion on the vibrational modes in amorphous silica by Legrand²² does not contradict the assignment of ν_4 to a stretching mode of a SiO_4 tetrahedron in which oxygen is substituted by an –OH or by –O–C. Furthermore, according to Zholobenko et al.,²³ the band at $1050 \pm 10 \text{ cm}^{-1}$ is related to the Q^3 silicon species since its intensity increases with the ratio Q^3/Q^4 . This band, at $1046 \pm 1 \text{ cm}^{-1}$ in Table 7, is 50% more intense in the gel than in the starting MCM-41. Etherification of Si–OH substitutes silanol by Si–O–CH₂–C–, but also new Q^3 silanols are formed by hydrolysis of siloxane bridges.²⁴ For details on the radial distributions, see ref 25.

(21) Herzberg G. *Molecular Spectra and Molecular Structure. II Infrared and Raman Spectra of Polyatomic Molecules*; Van Nostrand: New York, 1945.

(22) Legrand, A. *The Surface Properties of Silicas*; John Wiley: Chichester, 1998.

(23) Zholobenko, V. L.; Holmes, S. M.; Cundy, C.; Dwyer, J. *Microporous Mesoporous Mater.* **1997**, *11*, 83.

(24) Mertens, G.; Fripiat, J. J. *J. Colloid Interface Sci.* **1973**, *42*, 169.

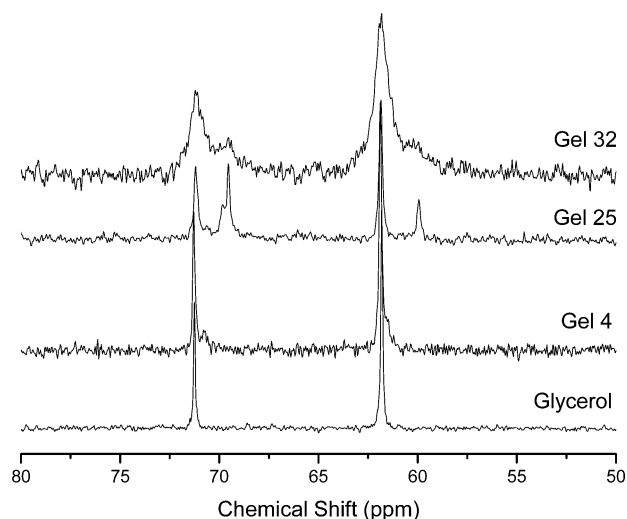


Figure 9. ^{13}C MAS NMR of glycerol, of gels 4 and 32 obtained from MCM-41, clinopt.SM, and gel 25 obtained from H ZSM5.

Table 7. Normalized Integrated Absorbance (Nabs, %) and Wavenumber (ν , cm^{-1}) of the Si–O Stretching Bands in Clinopt.SM and Gel 32

clinopt. SM		gel 32		assign
ν (cm^{-1})	Nabs (%)	ν (cm^{-1})	Nabs (%)	
943.7	9.3	945.9	2.7	n.a.
1047	18.4	1045	53.3	Si–OH, ν_3
1099	32.2	1097	24.7	Si–OH, ν_4
1162.5	19.5	1161	12.5	Si–O, s
1230	20.3	1219	7.4	

The interest of investigating the short range ordering by IR spectroscopy, in the framework of the present investigation, comes from the supplementary information obtained from the evaluation of the extent of etherification. Indeed, the assignment of a Si resonance line to $(\text{SiO})_3^*\text{Si}-\text{O}-\text{C}$ results from comparisons and not from a direct evidence. It will be shown in the conclusion that there is a reasonable linear fit between the ν_4/ν_3 ratio and the amount of substitutions $[(\text{SiO})_3^*\text{Si}-\text{O}-\text{subst}]/\text{Si}$ obtained from the deconvolution of the ^{29}Si NMR spectra, see eq 3.

Because the fate of the glycerol molecule is interesting, ^{13}C MAS, proton-decoupled NMR spectra were recorded. As represented in Figure 9, two resonances are observed at 61.8 ± 0.1 and at 71.3 ± 0.1 ppm, respectively, in glycerol. The most downfield is the most intense, the ratio of the integrated intensities being ~ 2 . These lines correspond to secondary and primary carbon, respectively. In gel 4, a weak new line appears at 71.1 ppm. The quasiconstancy of the shifts and of the intensity ratio shows that the integrity of the aliphatic carbon chain of the reacting glycerol is maintained in the gels derived from silica.

The quantitative description of the infrared spectra of clinoptilolite and of gel 32 is shown in Table 7. Again, bands ν_3 and ν_4 are present, the ratio ν_3/ν_4 being a measurement of the extent of the etherification reaction. The feldspars present in the raw material are involved neither in the depolymerization reaction nor the ammonium exchange.

Chemical Nature of the Gels Obtained from Synthetic HY and HZSM5 Zeolites. Three spectral regions can be delimited in the IR spectra: the characteristic vibrations of

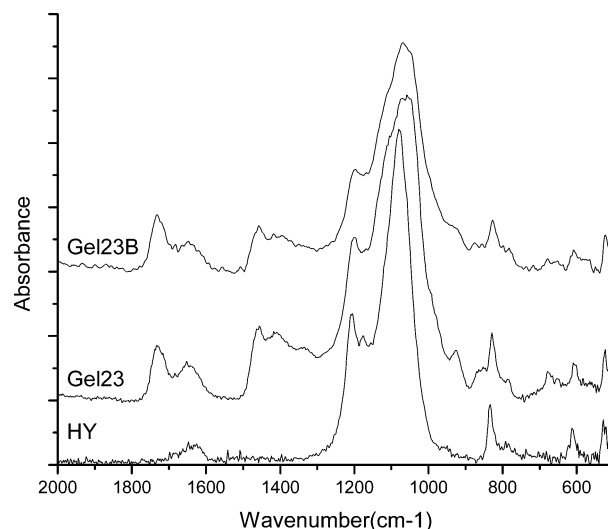


Figure 10. FT-IR spectra of HY and of the corresponding gels 23 and 23B.

Table 8. Deconvolution of ^{13}C MAS NMR Spectra^a

gels 2-4 and 44		gel 32		gel 25		glycerol	
δ (ppm)	int (%)	δ (ppm)	int (%)	δ (ppm)	int (%)	δ (ppm)	int (%)
		61.2	36.6	59.9	10.8		
61.8	66 ± 4	61.8	28.2	61.9	38	61.8	66
				69.6	21		
		69.8	18.2	69.9	8.4		
71.3	33 ± 3	71.2	(17)	71.2	21.8	71.3	33

^a Chemical shifts (δ , ppm), and relative intensity (int, %).

the organic groups are above 1200 cm^{-1} or below 1000 cm^{-1} , while the intermediate domain, shown in Figure 10, contains mostly the inorganic framework vibrations.

In the ^{13}C MAS NMR spectra of Figure 9, beside the two resonances attributable to the primary and secondary C atoms, two new lines, not observed in aluminum-free materials, appear upfield by about 2 ppm. The integrity of the glycerol carbon chain, observed in the gels derived from the silica, is no longer respected in the gels obtained from aluminosilicates. Also, a new band near 1735 cm^{-1} appears in the IR spectra of gels 23 and 23B in Figure 10. In saturated esters,²⁶ the C=O stretching is strong and between 1735 and 1750 cm^{-1} , and the ^{13}C resonance is upfield,²⁷ as shown in Table 8. The interpretation is the transformation of alcohol functions into easily oxidized carboxylic groups mediated by the strongly acidic Al–OH–Si group. Also, in these gels the formation of a small amount of black material, probably linked to an oxidation process, is observed.

If the lines at 59.9 and 61.9 ppm are attributable to primary carbons whereas the lines at 69.6, 69.9, and 71.2 ppm are related to secondary carbons, the intensity swap observed in gel 25 would favor the hypothesis of an enhanced activity of the glycerol secondary alcohol group toward etherification.

Chemical Composition. Because the reaction product is a gel dissolved in an excess of glycerol, the chemical analysis

(25) Ratnasamy, P.; Leonard, A. J. *Catal. Rev.* **1972**, 6 (2), 293.

(26) Bellamy, L. J. *The Infrared Spectra of Complex Molecules*; Methuen: London, 1958.

(27) *Selected NMR Spectral Data*; American Petroleum Institute, project 44, Texas A&M Research Foundation, 1966.

Table 9. C/Si Atom Ratio and % Porosity Volume Filled by the Organic Residues

	gel 9	gel 10	gel 11	gel 15	gel 17	gel 44	gel 25	gel 23	gel 23B
C/Si	3.04	3.35	3.57	1.14	1.62	0.6	0.81	0.99	1.17
porosity	75	77	79	54	63	38	45	50	53

must distinguish the organic residues, attached to the inorganic framework from the solvent, e.g., the excess glycerol. The weight loss between 25 and 325 ± 10 °C is due to the removal of the hydration water and of the excess glycerol; the latter is marked by a sharp endothermic peak between 200 and 300 °C. Above this temperature and up to 1000 °C, the organic fraction of the gel is removed. Beyond 1000 °C, the residue is dehydrated SiO₂. A broad and weak exothermic peak, observed near 450 °C, is probably due to the oxidation of the organic matter.

Let P_1 and P_2 be the percent remaining weights at 300 and 1000 °C, respectively. The weight percent solvent in the material is $(100 - P_1)$, and the weight percent silica in the gel is $MP_1 = m_g$, where M is the total weight of analyzed material, including the excess glycerol.

The gel contains an organic (m_{org}) and an inorganic fraction (m_{inorg}). From the definition follow

$$m_{\text{inorg}} = P_2 M / 100 \text{ and } m_{\text{org}} = (P_1 - P_2) M / 100 \quad (1)$$

The C content is approximated by $m_{\text{org}}/30$ where 30 is the molecular weight of the H-C-OH fragment representing the structural unit of the organic residue. The weight of the gel is $(m_{\text{inorg}} + m_{\text{org}})$, and the yield of the depolymerization reaction is $(m_{\text{inorg}} + m_{\text{org}})/M$. The SiO₂ content in the gel is $m_{\text{inorg}}/60$. Some results are shown in Table 9.

The porous volume occupied by organic material/g SiO₂ in the gel can be roughly approximated as $m_{\text{org}}/1.2613/m_{\text{inorg}}$, 1.2613 being the specific volume of glycerol at 20 °C. These porous volumes, shown in Table 9, are of the order of magnitude of the actual pore volumes measured by N₂ physical adsorption. For MCM-41 and FSM-16 [5, 17, 30], they are between 0.6 and 1 cm³/g.

Because of the paramount importance of the silanol in the depolymerization reaction, the OH surface concentration in the precursor should play an important role. Several techniques for measuring the OH surface density in silica were proposed and reviewed in the past by Little.²⁹ Davidov, Kiselev, and Zhuralev³⁰ measured the OH surface density by four different techniques for a large number of silicas with surface areas between 750 and 40 m²/g. On these materials, the average results expressed as the surface density (OH molecules/nm²) obey an empirical equation

$$\text{OH/nm}^2 = -2.46 + 3.580/T (\text{K}) \pm 0.2 \quad (2)$$

(28) Brinker, C. J.; Scherer, G. W. *Sol-Gel Science. The Physics and Chemistry of Sol-Gel Processing*; Academic Press, Inc.: New York, 1990.

(29) Little, L. H. *Infrared Spectra of Adsorbed Species*; Academic Press: New York, 1966; see chapter by Kiselev and Lygin, p 275.

(30) Davidov, V.; Kiselev, A. K.; Zhuravlev, L. T. *Trans. Faraday Soc.* **1964**, *60*, 2254.

Table 10. OH/Si and OH/nm² Ratios from Equation 3^a

sample	Q ² %	Q ³ %	Q ⁴ %	subs/ Si=OH/Si	A (m ² /g)	OH/ nm ² ^b	OH/ nm ² ^c	C/ Si
FMS-16	5.2	6.5	88.3	0.169	847	2.0	3.6	1.62
MCM-41	5.7	15.4	78.8	0.268	849	3.2	2.3	1.14
xerogel	6.3	32.7	61.0	0.453	428	10.6	8.4	0.6

^a A = BET specific surface area, (m²/G), OH/nm² from weight loss. In the last column, C/Si ratio in gels 17 (top), 15 (next), and 44 (bottom).

^b From eq 3. ^c From weight loss.

The deconvolution of the ²⁹Si MAS NMR spectra into its components Q⁴, Q³, and so forth, permits the calculation of the average number of substitutions per Si. The following equation applied successfully to the Al/Si substitutions¹³ in zeolites, is used:

$$\frac{\text{Si}}{\text{subst}} = \frac{\sum_{m=0}^{m=4} I(Q^m)}{\sum_{m=0}^{m=4} (m/4)I(Q^m)} \quad (3)$$

in order to calculate the OH surface density of MCM-41 and FSM-16. A strict rule such as the Loewenstein rule, observed for the Si/Al substitutions, is not necessarily obeyed by the hydroxyls. Nevertheless, the Si(OH)₂ population is always small.²²

The gel TGA diagram contains, after the removal of hydration water near 100 °C, a broad peak, ca. 270 °C due to the surfactant removal (except for gel 44) and near 350 °C a sharp peak attributable, in part, to the dehydroxylation of the surface. The surface density obtained from the high temperature (>390 °C) weight loss and the value obtained from empirical eq 2 follow the same trend, Table 10. According to eq 2, at 590 °C, the average OH surface density is $1.9 \pm 0.5/\text{nm}^2$, and it is $7.1 \pm 0.5/\text{nm}^2$ at 373 K.

Discussion

The first step of the depolymerization reaction of MCM-41 may be tentatively schematized as the etherification of the weakly acid silanol group by an alcohol function of glycerol (maybe the secondary). A water molecule is formed, and at ~200 °C, it hydrolyzes an adjacent Si-O bond, generating new hydroxyls, eventually able to react with nearby glycerol. A new molecule of water is formed, and a chain of autocatalytic reactions propagates through the whole lattice in pores available to glycerol and fitted with silanols. Similar observations were made in measuring directly the surface concentrations of surface methoxy groups and silanols in the reaction of methanol with an aerogel.²⁴ Because of the opening of siloxane bridges, the final C/Si is always smaller than the initial OH/Si.

The value of the average atomic ratio C/Si depends on the extent of etherification, on the condensation of the organic residue fixed on the silica, that is to say, on the distribution of [Si-O-Si, $n(\text{OCH})$] units of different sizes. The theoretical maximum value of C/Si is 4. If this value was ever

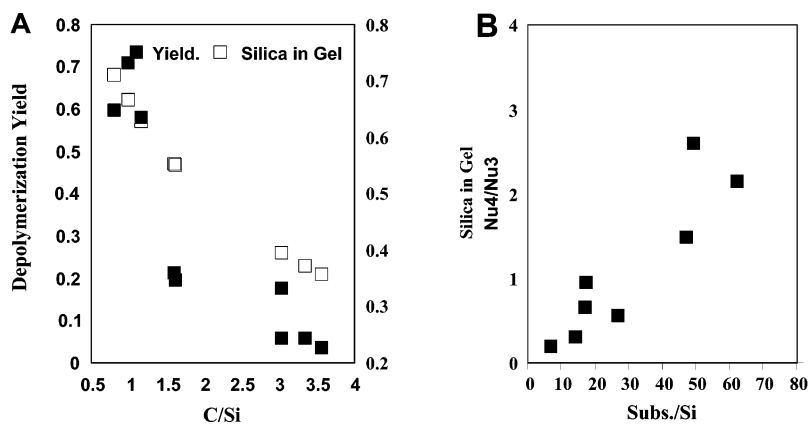


Figure 11. (A) Decrease of the yield of the depolymerization reaction and of the amount of silica in the gel with increasing C/Si. (B) Variation of the IR ratio ν_4/ν_3 with respect to the number of substitutions per Si, obtained from ^{29}Si MAS NMR.

reached, it would mean that the original structure is transformed into monomeric tetrahedral units of about 0.26 nm^3 .

On the other hand, the observation of tetrahedral aluminum in zeolitic gel permits an estimation of the size of the smallest structural unit in the gel. For instance, in a near faujasite HY gel 23, where there are 12.7 tetrahedral units per nm^3 and where the Si/Al ratio is 12.9, the smallest structural unit must be about 1 nm^3 . By the same token, this volume should be 1.24 nm^3 in gel 25, from HZSM-5. In these nanovolumes, the local structural ordering must be very much the same as in the starting materials, as suggested by the similitude of the ^{29}Si and ^{27}Al MAS NMR spectra. The internuclear distances and bond angles must remain almost constant in the neighboring coordination shells. At larger scales, the disorder resulting from misfits in the distribution of the elementary structural units increases, resulting in the amorphization of the material. Because of the residual organization, it is likely that the gels would work efficiently as seeds in secondary syntheses, whereby the gels would be used as a source of silica and alumina.

The reaction time, temperature, and initial composition contribute to the gel properties. Acid-catalyzed TEOS hydrolysis studies reported by Brinker and Scherer²⁸ illustrate the possible pathways of gel syntheses. Depending upon the duration of the contact with the hot glycerol, the temperature, and the yield of the reaction (Table 3), the degree of substitution varies between broad limits. It is observed systematically that a high degree of substitution corresponds to a lower production of gel.

The links between the four series of independent measurements characterizing the reaction are summarized in Figure 11. The C/Si ratio is related to the yield of the depolymerization reaction, and to the silica content of the gel, Figure 11A, it was found that the lower C/Si is, the larger the yield is. The SiO_2 content in the gel decreases quasilinearly as the C/Si ratio increases, as expected.

The spectroscopic techniques, ^{29}Si MAS NMR and IR, point to the local ordering of the gel building elements, Figure 11B. In Figure 11B, the ratio of the intensity of the stretching vibrational modes (ν_3/ν_4) of the silicon tetrahedron and the ratio C/Si increase with the progress of the reaction, estimated from the intensity of the NMR lines associated to the silicon Q^2 and Q^3 clusters.

The partial oxidation of glycerol into a carboxylic acid, followed by etherification of the acid function, evidenced by the ^{13}C MAS NMR in Figure 9 and the IR spectra in Figure 10, and the observation of a larger yield of the depolymerization reaction, are typical of the zeolites. Both sets of observations may be linked to the strong acidity of the zeolite OH acid sites, subsisting in the gels.

The gels keep appreciable pore volumes filled by the organic material fixed on the silicate frameworks, Table 10.

Conclusion

Mesoporous MCM-41 and FSM-16 crystalline silicas, xerogel, natural and synthetic zeolites, clinoptilolite, H-faujasite, and H-ZSM-5 depolymerize rapidly (reaction time $< 2 \text{ h}$) in glycerol in the temperature range ca. $200 \text{ }^\circ\text{C}$. The reaction product is a gel made from silica clusters containing Si–O–C substitutions and dissolved in an excess of unreacted glycerol. Some organization of the structural elements, silicon tetrahedra or aluminum tetrahedra, subsists in the gels. Likely, all large surface area silicates, amorphous or crystallized, containing silanol groups would behave similarly.

Acknowledgment. We thank Professor P. Bosch, UNAM, Mexico, for the gift of clinoptilolite, Professor G. Poncelet, University of Louvain, Belgium, for the sample of xerogel, and IMP (Project D.00145) for financial support and for the permission to publish.

IC050562P